Intrusion Location with Breaking-the-Pulse-Width-Limit Spatial Resolution and High Robustness based on φ-OTDR and Spatial Frequency Analysis

Zhou Sha, Hao Feng, Yi Shi and Zhoumo Zeng

State Key Laboratory of Precision Measurement Technology and Instruments, School of Precision Instrument and Opto-electronic Engineering, Tianjin University, 92 Weijin Road, Tianjin 300072, China

Keywords: Phase-sensitive OTDR, Vibration Location, Spatial Resolution, Spatial-frequency, Energy Distribution.

Abstract: This paper proposes a vibration location method based on spatial-frequency analysis, which can help achieve better location performance in the application of φ-OTDR. The method is proven to be able to separately locate coupled vibration events to some extent, achieve break-the-pulse-width-limit spatial resolution in the case of single event detection with higher robustness, and provide more comprehensive information about the vibration situation to better identify vibration events, noise and disturbance. Different experiments including indoor and outdoor tests are conducted to practically validate the effectiveness of the method and its advantages over the conventional moving differential method. Experiment results show that the proposed method exhibits several useful merits.

1 INTRODUCTION

Distributed optical fibre sensing technique based on phase sensitive Optical Time Domain Reflectometry (Taylor and Lee, 1993) has become increasingly popular in recent years (Bao and Chen, 2012). With the capability of simultaneous multipoint monitoring, easiness of deployment and maintenance, intrinsic immunity to chemical corrosion and electromagnetic interference as well as the cost effectiveness, φ-OTDR has been extensively used in many fields such as intrusion detection, perimeter security surveillance (Owen et al., 2012), oil and gas pipeline monitoring (Peng et al., 2014a), railway safety monitoring(Peng et al., 2014b), structural health monitoring (Bahrampour et al., 2010) as well as seismic applications. Many researches have been conducted to improve the sensing performance from different perspectives, such as extending the sensing range from typically tens of kilometres to over 100km (Wang et al., 2014), raising the frequency response to break the round-trip-time limit (He Q et al., 2015), overcoming the nonlinear distortion of intensity detection by conducting phase demodulation and so forth (Wang et al., 2016).

Although the performance of φ-OTDR has been greatly improved from many perspectives (Wu et al. 2015), the research pertaining to enhancing the capability of vibration location is rather limited. Since having the vibration events located is generally fundamental and prior to other subsequent analysis, it is necessary to spend efforts improving the location capability. Traditional ways of locating intrusions include moving differential (Lu et al., 2010) and distributed parameter computation (Shi et al., 2016), which both have their noticeable drawbacks. The working principle of moving differential is based on the time signal fluctuation. It picks out those positions with high fluctuation amplitude as the results of intrusion location. Since the laser frequency drift and environmental temperature change can also cause signal fluctuations, fake differential peaks and false location results can be generated when moving differential is used in practical applications. The distributed parameter computation computes some parameter of the time signal in each position as an indicator of the presence of intrusion. The parameter can be selected from the perspective of statistics and information theory, such as entropy and correlation dimension (Shi et al., 2016). Although this method generally gives a better location performance

17

compared to moving differential, the computation load is somehow raised in a significant level, regardless of which specific indicator is chosen. As a consequence, real time monitoring is unachievable and the method can hardly be applied in practical applications. On the other hand, the spatial resolution is limited by the probe pulse width. Higher pulse width would lead to lower spatial resolution, thus deteriorates the location accuracy.

Our work proposed a new vibration location method using spatial frequency analysis. It reports the vibration condition in the entire sensing range in a straightforward and intuitive way. The energy distribution along the fibre of each frequency component and the power spectrum at each position are simultaneously reflected in one colour-encoded figure. Since vibrations in different frequency bands are independently presented at different positions along the frequency axis, fake fluctuations caused by laser frequency drift and environmental temperature change, which more often appears with lower frequency, can be conveniently distinguished and thus will not lead to confusion. Besides, thanks to the Fast Fourier Transform algorithm, this method based on spatial frequency analysis is high-efficiency and time-saving. In addition, combined with the results of Shi et al., (2015), this method can explicitly determine the edge of the vibration segment, thus realize break-the-pulse-width-limit spatial resolution for single event detection with higher robustness. For overlapped multiple vibration events with unique power spectrum, this method can also help separate the events to a certain extent, and thereby achieve higher general spatial resolution.

2 METHODOLOGY

The principle of the proposed spatial-frequency analysis is illustrated in Fig. 1. The blue matrix is essentially composed of multiple time-aligned Rayleigh backscattered (RBS) traces, with the horizontal axis being spatial location and the vertical axis being time. Performing FFT transform vertically to the blue matrix yields the red matrix, which presents the energy distribution with respect to space and frequency. Different columns of the red matrix represent the power spectrum density at different positions. Different rows of the red matrix represent the energy distribution of different frequency components along the fibre. As can be seen, with the help of this frequency-spatial energy distribution matrix, one can easily and intuitively obtain the frequency information at each location.

The position without vibration would exhibit low-level and uniform energy distribution, yet the position affected by external vibration would exhibit unique power distribution pattern, which is essentially the power spectrum. Thus, vibration events can be easily located by inspecting the energy distribution simultaneously in the spatial and frequency domain.
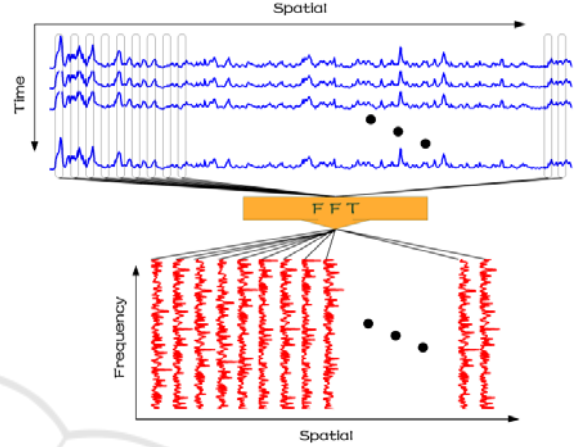

Figure 1: Principle illustration.

Assume the length of the sensing fibre is L, the sampling rate of the data acquisition card is f, the pulse repetition rate is N, the refractive index of fibre is n, and the raw data matrix (blue matrix) is made up of data generated within one second, then the raw data matrix can be expressed as

$$I = \left(T_1 \ \ T_2 \cdots \ T_i \cdots T_M \right)^T \qquad (1)$$

$$T_i = [\mathrm{S}_{i1} \ \mathrm{S}_{i2} \ \cdots \ \mathrm{S}_{iM}] \qquad (2)$$

$$M = 2nfL / c \qquad (3)$$

T_i, which is made up of M sample points, denotes the ith RBS trace. By concurrently performing FFT to each column of I, the spatial-frequency energy distribution matrix is generated and expressed as

$$O = \left(F_1 \ \ F_2 \cdots \ F_j \cdots F_N \right) \qquad (4)$$

$$F_j = [\mathrm{A}_{1j} \ \mathrm{A}_{2j} \ \cdots \ \mathrm{A}_{Nj}]^T \qquad (5)$$

F_j is the power spectrum of time signal S_j. The value of A_{ij} is calculated by means of FFT algorithm,

$$A_{ij} = \sum_{k=0}^{N-1} S_{kj} \cdot w_N^{ik}, \quad w_N^i = e^{-\mathrm{i}2\pi i/N} \qquad (6)$$

where i is the imaginary unit, i is the discrete frequency index. This allows us to obtain the spatial

distribution of each and every discrete frequency component i,

$$D_i = [A_{i1}\ A_{i2}\ \cdots\ A_{iM}]\qquad(7)$$

D_i denotes the spatial energy distribution of discrete frequency i.

The method is essentially mapping the signal energy into a spatial-frequency plane from which one can independently investigate each discrete frequency's distribution along the fibre and the unique power spectrum of time signal in each position. One such colour-encoded plane provides the general view of the entire sensing range in one second. Positions with vibration can be distinctly revealed, and its specific power spectrum is at the same time readable. Low frequency fluctuation caused by laser drift and temperature change will only appear in the low frequency band, and the positions with real vibration will have unique energy distribution in the high frequency band. Thus the fake vibration can be distinguished from the real ones by looking at the spatial-frequency energy distribution pattern and inspecting the frequency band they occupy.

3 EXPERIMENTAL VALIDATION

In order to validate the effectiveness of the method, different experiments including indoor and outdoor vibration tests are conducted where the vibration events are located using the proposed spatial frequency analysis. The system setup is shown in Fig. 2. An NKT ultra narrow line width laser is used as the light source. The continuous seed light is modulated into pulses with an Acoustic Optic Modulator (AOM). After that, the pulses are boosted by an Erbium Doped Fibre Amplifier (EDFA) to obtain higher peak power. A Fibre Bragg Grating (FBG) is employed together with an optical circulator to filter out the Amplifier Spontaneous Emission (ASE) noise from EDFA. A second AOM is applied right after the FBG to enhance the Extinction Ratio (ER). The pulsed probe light is injected into the sensing fibre through an optical circulator and the Rayleigh Back Scattered light (RBS) is detected with a PIN detector. The signal is sampled with a 50MS/s Data Acquisition Card (DAC) and processed subsequently in a computer.

Three types of vibrations, respectively caused by Piezoelectric Transducer cylinder (PZT tube), striking the steel plate and water pipe leakage are
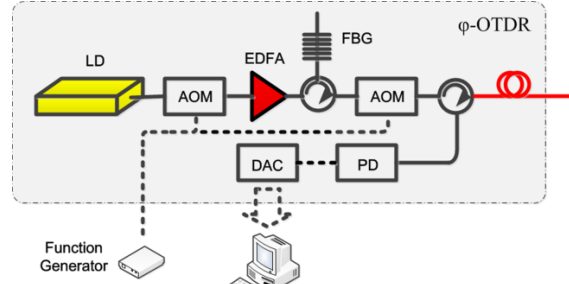
measured with the φ-OTDR system.

Figure 2: Experimental setup ф-OTDR structure.

3.1 PZT Vibration Test

Firstly, two PZT tubes are used to apply sinusoidal vibration to the fibre. A function generator drives the two PZT tubes with the corresponding frequency being 170Hz and 70Hz. The fibre's length between the two PZT tubes is 6m. A schematic diagram of the deployment structure is illustrated in Fig. 3.
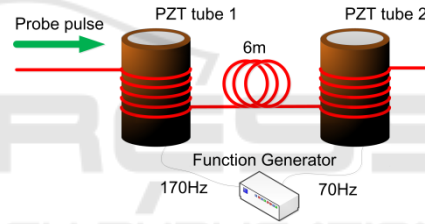

Figure 3: PZT vibration setup.

The vibration caused by the two PZT tubes are firstly located using the conventional moving differential method. The location result is shown in Fig. 4.
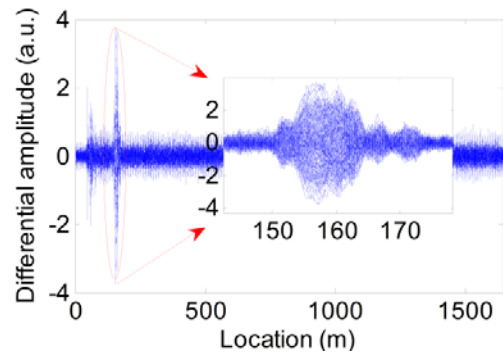

Figure 4: Moving differential traces.

It can be observed from Fig. 4 and the inset that a differential peak appears at around 160 m, which indicates the presence of vibration event at the

mentioned location. The 160m location result is basically correct, however, the starting point of the vibration segment is not sufficiently clear. The two individual vibration events respectively caused by the two PZT tubes with different frequency can not be distinguished. This partly exhibits the intrinsic drawbacks of the moving differential locating algorithm.

As comparison, the proposed spatial frequency analysis is performed on the same set of experiment data, and the location result is shown in Fig. 5 and Fig. 6, which are essentially colour-encoded energy distribution matrix, describing how the signal energy is distributed with respect to space and frequency. From Fig. 5 it can be observed that there is an concentrated energy distribution around the position 160m. The corresponding frequency range at that position approximately starts from 0Hz and ends at 1kHz. Zooming in Fig. 5 gives us Fig. 6, which clearly exhibits the frequency distribution pattern of the vibration in detail. Based on Fig. 6 we are allowed to infer the presence of two individual vibration events.
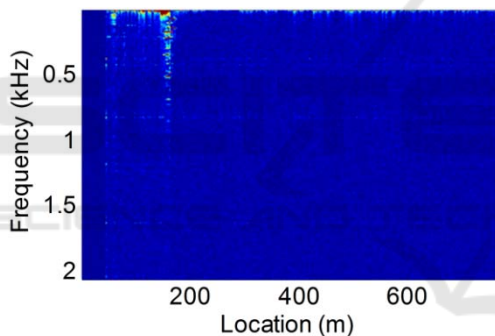

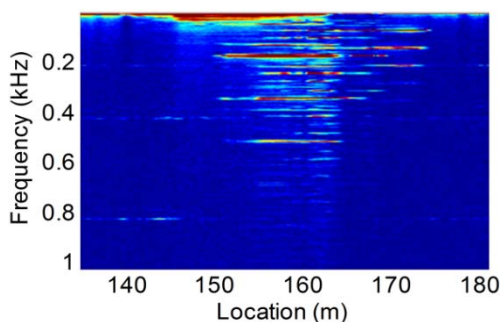Figure 5: Spatial frequency energy distribution.

Figure 6: Spatial frequency energy distribution (detail).

The three thick lines horizontally starting from 150m, vertically appearing at 170Hz, 340Hz and 510Hz are all caused by the 170Hz PZT vibration, where the 340Hz line and 510Hz line appear as a result of the interference induced nonlinear

distortion of intensity signal. The four lines horizontally ending at about 175m, vertically appearing at 70Hz, 140Hz, 210Hz and 280Hz are caused by the 70Hz PZT. Similarly, the three lines apart from the 70Hz line are present due to the interference induced nonlinear distortion, which can be mathematically explained by the Jocobi-Angry expansion. Therefore, the processing result of the proposed spatial frequency analysis is able to provide a much larger volume of information than moving differential can do. It helps distinguish coupled vibration events based on their unique frequency distribution patterns. Besides, by synthetically taking into account the emergence position of each frequency component, one can determine the staring point of the vibration segment with higher robustness. It is revealed from the research results in [3] that the starting point of the vibration segment on the intensity trace is the real indication of the vibration location. In the case of single event detection, distinctly determining the starting point of vibration segment means one can achieve spatial resolution that breaks the pulse width limit. Therefore, the proposed method can also help locate single vibration event with higher accuracy and spatial resolution that is decoupled with the probe pulse width.

Based on the results given in Fig. 6, we can infer that 170Hz and 70Hz are the two characteristic frequency components that can be used to reveal the respective positions of the two vibration events. Thus the energy distribution along the fibre of the two characteristic frequency components are extracted and plotted in Fig. 7. Two peaks with rather high signal to noise ratio are clearly present at around 160m. From the inset, it can be seen the two peaks respectively start from 151m and 157m. The 6m interval agrees well with the fibre length between the two PZT tubes.
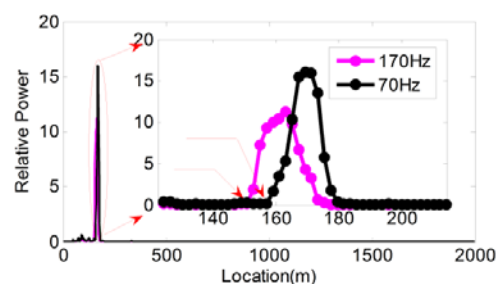

Figure 7: Spatial distribution of characteristic frequencies.

3.2 Steel Plate Striking Test

For the purpose of testing the location performance

of the proposed method in practical vibration condition, the second experiment is designed where a steel plate struck by a hammer is used as the vibration source. The deployment schematic diagram is shown in Fig. 8. The fibre is coupled with the steel plate by vacuum coupling agent which assures better plate-fibre vibration transmission. The steel vibration signal is monitored using the home made φ-OTDR system as shown in Fig. 2 and is firstly located using the conventional moving differential method with the result shown in Fig. 9. A peak can be found at around 155m on the differential trace, which indicates the presence of vibration event. As can be seen from the inset, the peak's starting point is not clear and the signal to noise ratio is rather low, thus the vibration location can not be accurately determined.

The same experiment data is then processed using the proposed spatial frequency analysis and the location result is shown in Fig. 10. A vertical line at around 150m is explicitly shown. Having the line and its vicinity zoomed in and shown in the inset, the starting position can be accurately determined to be 150m. Besides, the frequency component of the vibration is at the same time revealed. The energy is shown to cover the entire frequency response range, *i.e.*, 0-2.5kHz.

Figure 8: Striking steel plate.

Based on the information given in Fig. 10, the power spectrum of the signal at 150m is plotted to further investigate the energy distribution, which is shown in Fig. 11. Four maximum frequency components, respectively 93Hz, 204Hz, 387Hz and 705Hz are picked out as the characteristic frequencies of the vibration event. The energy distribution of the four characteristic frequencies along the sensing fibre are plotted in Fig. 12. It can be observed that the energy level of each of the four frequency components reaches its maximum value within the range of 150m to 160m. Therefore, the spatial energy distribution of each of the four characteristic frequencies can be used to determine the vibration location.
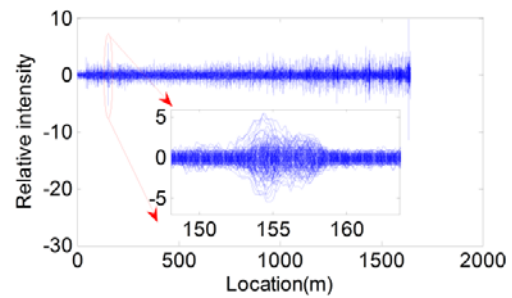

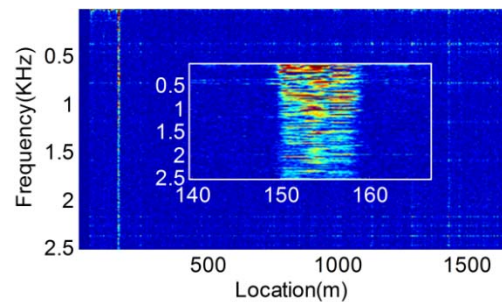Figure 9: Moving differential traces.

Figure 10: Spatial frequency energy distribution.

This part of the experiment results show that the proposed spatial frequency analysis can provide more abundant information to help locate and identify the vibration event, such as revealing the frequency spectrum, indicating the characteristic frequency, explicitly and robustly give the start position of the vibration segment.
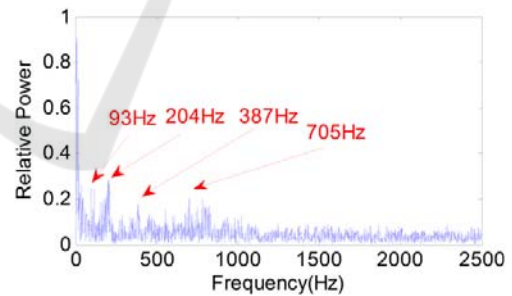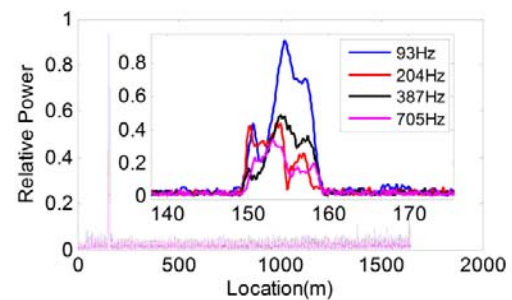

Figure 11: Characteristic frequencies.

Figure 12: Spatial distribution of characteristic frequencies.

3.3 Pipe Leakage Vibration Test

Pipeline integrity monitoring is one of the major applications of φ-OTDR, where the detection and location of external intrusion and pipeline accident such as pipe leakage is necessary. An experiment pertaining to pipeline leakage location is designed using the home made φ-OTDR system and conducted inside a greenhouse. The field setup is schematically shown in top view in Fig. 13. A PE water pipe is buried under ground, with about 15m of it immerged in a dug water tank. An 8mm hole is drilled on the pipe shell to simulate pipe leakage. A water pump is used to pump the water from a water well into the water pipe. The sensing fibre is glued on the pipe shell surface. When the water pump comes into operation, water leakage would occur through the leakage hole, and the leakage induced vibration is monitored by the sensing fibre.
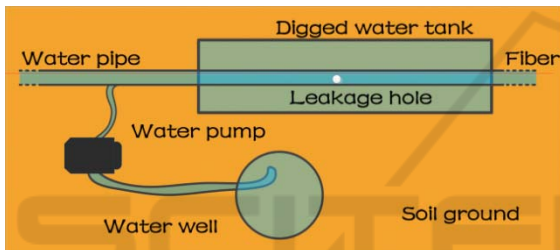

Figure 13: Pipeline leakage experimental setup.

The leakage event is respectively located using the conventional moving differential method and the proposed spatial frequency analysis. The processing result of moving differential is presented in Fig. 14 and Fig. 15. A conspicuous peak appears at around 650m in Fig. 14, which basically gives the correct position of the leakage event. However in Fig. 14 where the differential peak is zoomed in for clearer observation, it is hard to tell the starting point of the vibration segment in that an explicit bound between the peak and the background trace can hardly be found. Therefore, the location accuracy is rather limited.

By performing the proposed spatial frequency analysis, the leakage event could be better located with higher accuracy. Fig. 16 gives the spatial frequency energy distribution in a full view. The energy line at about 650m reveals the correct leakage position. In Fig. 17 the energy line is zoomed in where the start position of vibration segment can be explicit determined. It can be observed according to the part of line vertically from 300Hz to 500Hz that the precise start point is 657m. Disturbance are present in the frequency range

below 200Hz, mainly in 50Hz, 100Hz and 150Hz. This noise is validated to be caused by the water pump. When the water pump engine is turned on, the disturbance accordingly comes about. When the water pump engine is turned off, the disturbance disappears.
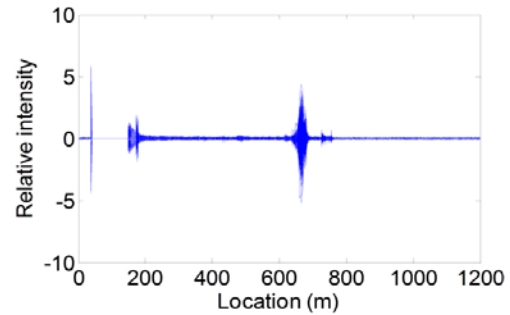

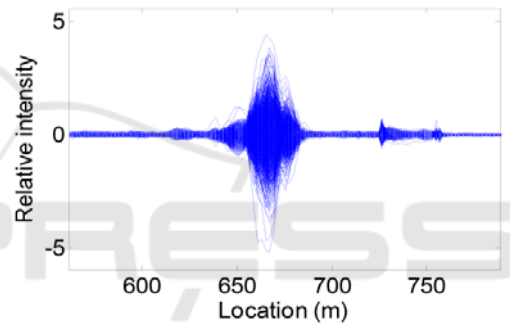Figure 14: Moving differential traces.

Figure 15: Moving differential traces (detail).

In general, based on the spatial frequency energy distribution, one can clearly observe the presence of the disturbance caused by the water pump engine vibration, accurately determine the leakage position by referring to the part of energy distribution over 200Hz and even identify those positions that are contaminated by the water pump engine noise. Spatial frequency energy distribution provides more useful and comprehensive information about the vibration situation in the monitoring field and thus helps achieve better location performance.
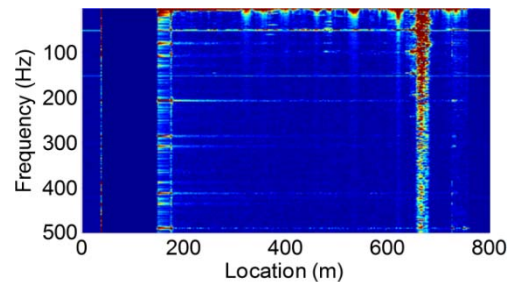

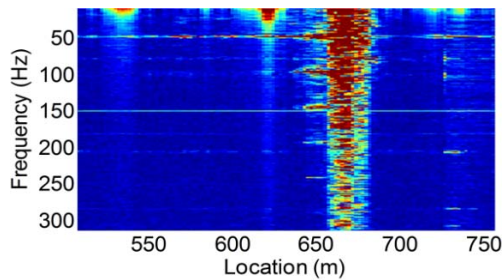Figure 16: Spatial frequency energy distribution.

Figure 17: Spatial frequency energy distribution (detail).

4 CONCLUSIONS

A vibration location method used in φ-OTDR system based on spatial frequency analysis is proposed and demonstrated. Different experiments including indoor and outdoor tests are conducted to comprehensively evaluate the method's locating performance in different situations. The method has been proven to exhibit several useful advantages over the conventional moving differential method. Firstly, it provides vibration information in a more comprehensive way. By referring to the vibration energy distribution with respect to space and frequency, one can easily achieve an intuitive comprehension about the vibration condition in the entire sensing range. The colour-encoded image can conveniently reflect how the energy is distributed in the frequency domain in each position and how the energy of each frequency component is distributed along the fibre. Vibration caused by different sources can be separated according to their unique frequency spectrums. By synthetically considering the emerging position of each frequency component, one can determine the start position of vibration segment in a more accurate and robust way, which will lead to better location results. According to the research result reported in (Shi et al., 2015), it is the start point of the vibration segment that reveals the real vibration location, thus accurately determining the border of vibration segment is of great importance in that the pulse width limit upon the spatial resolution can be broken through. Therefore this method can help achieve break-the-pulse-width-limit spatial resolution with higher robustness.

Apart from the location information, the frequency spectrum of each detected vibration is reflected at the same time. Since vibration caused by different sources generally exhibit different characteristic in the frequency domain, this property is thus very useful to help identify different vibrations.

Besides, thanks to the mature application of the FFT algorithm, the proposed method can be performed in a very convenient and time-saving way. Real time monitoring based on the proposed method is generally available.

REFERENCES

H. F. Taylor and C. E. Lee, 1993. Apparatus and method for fibre optic intrusion sensing. *U.S. Patent* 5194847.

X. Bao and L. Chen, 2012. Recent progress in distributed fibre optic sensors. *Sensors (Basel)* 12(12), 8601–8639.

Shi. Y et al., 2015. A long distance phase-sensitive optical time domain reflectometer with simple structure and high locating accuracy. *Sensors (Basel)* 15(9), 21957–21970.

Wu. H et al., 2015. Separation and determination of the disturbing signals in phase-sensitive optical time domain reflectometry (Φ-OTDR). *J. Lightwave Technol.* 33(15), 3156–3162.

Peng. F et al., 2014a. Ultra-long high-sensitivity Φ-OTDR for high spatial resolution intrusion detection of pipelines. *Opt. Express* 22(11), 13804–13810.

Peng. F et al., 2014b. Real-time position and speed monitoring of trains using phase-sensitive OTDR. *IEEE Photonics Technol. Lett.* 26(20), 2055–2057.

Owen, G. Duckworth and J. Worsley, 2012. Fibre optical distributed acoustic sensing for border monitoring. *2012 European Intelligence and Security Informatics Conference*, 362–364.

Shi. Y et al., 2016. Correlation dimension locating method for phase-sensitive optical time domain reflectometry. *Optical Engineering*, 55(9): 091402-091402.

Bahrampour A R et al., 2010. Resolution enhancement in long pulse OTDR for application in structural health monitoring. *Optical fibre technology*, 16(4): 240-249.

Wang. Z et al., 2014. Ultra-long phase-sensitive OTDR with hybrid distributed amplification. *Optics letters*, 39(20): 5866-5869.

He. Q et al., 2015. Frequency response enhancement by periodical non-uniform sampling in distributed sensing. *IEEE Photonics Technology Letters*, 27(20): 2158-2161.

Wang. Z et al., 2016. Coherent Φ-OTDR based on I/Q demodulation and homodyne detection. *Optics express*, 24(2): 853-858.